1661-8726/07/020313-12
DOI 10.1007/s00015-007-1219-z
Birkhäuser Verlag, Basel, 2007

Swiss j. geosci. 100 (2007) 313–324

U-Pb SHRIMP zircon dating of andesite from the Dolomite area (NE Italy): geochronological evidence for the early onset of Permian Volcanism in the eastern part of the southern Alps

DARIO VISONÀ[1], ANNA MARIA FIORETTI[2], MARIA ELIANA POLI[3], ADRIANO ZANFERRARI[3] & MARK FANNING[4]

Key words: Permian, andesite, SHRIMP age, Athesian Volcanic District, NE Italy

ABSTRACT

The Athesian Volcanic District (AVD), a thick sequence of andesitic to rhyolitic lava and ignimbrite, overlies both the Variscan basement of the Dolomites and, where present, the continental basal conglomerate of Upper Carboniferous(?) to Early Permian age. This volcanic activity is known to mark the margin of the intra-Pangea megashear system between Gondwana and Laurasia, the onset age of which is determined in this study.

SHRIMP U-Pb dating on zircon from Ponte Gardena/Waidbruck (Isarco/Eisack valley) basaltic andesite yields an age of 290.7 ± 3 Ma, providing the oldest record of andesite volcanic activity yet documented in the AVD. Two younger dates (279.9 ± 3.3 and 278.6 ± 3.1 Ma) obtained for the andesitic necks of M. dei Ginepri (Eores/Aferer valley) and Col Quaternà (western Comelico), respectively, probably represent a second pulse of andesite magmatic activity.

Near Chiusa/Klausen, the volcanoclastic deposits at the bottom of the Funes/Villnöss valley volcano-sedimentary complex only contain detrital zircons, dated at 469 ± 6 Ma; these probably derive from erosion of Paleozoic porphyroids. Other zircons from the same sediments and inherited cores of magmatic andesite crystals give Paleoproterozoic (1953.6 ± 22.1, 1834.6 ± 69.3, 1773.6 ± 25.1 Ma), Early Neoproterozoic (1015 ± 14 Ma) and Late Neoproterozoic (728.4 ± 9.6, 687.6 ± 7.6 Ma) ages. These ancient detrital and inherited zircon ages fit the model that envisages the Dolomite region as being tectonically coherent with Africa, at least until the Lower Permian.

Introduction

Permian magmatism in the Dolomite region involves both intrusive complexes, ranging in composition from gabbro to granite (Bressanone-Ivigna-Chiusa, Cima D'Asta) and large volumes of volcanic rocks (Athesian Volcanic District – AVD), with compositions ranging from basaltic andesite to rhyolite (Bonin et al. 1993; Rottura et al. 1998). This magmatism occurs at the margin of the intra-Pangea dextral megashear system between Gondwana and Laurasia which, during the Early Permian, transformed Pangea "B" into Pangea "A" (see Muttoni et al. 2003). According to this model, the Adriatic plate, including the Dolomite region, was tectonically coherent with Africa (Gondwana) and was located south of the megashear zone. The geochemical character of the magmatic products does not reflect the above tectonic environment, as gabbro and basaltic andesite have a marked orogenic signature. To explain this apparent discrepancy, an inherited mantle source has been assumed, which was geochemically modified by previous subductions (Rottura et al. 1998).

The age of the onset of magmatic activity has not been clearly defined, in spite of numerous radiometric and biostratigraphic efforts (e.g., Del Moro & Visonà 1982; D'Amico & Del Moro 1988; Barth & Mohr 1991). For the plutons, there seems to be a polarity with slightly older ages towards the NW (275 Ma, Cima d'Asta; 282 Ma, Bressanone; 301 Ma, Ivigna; Sassi et al. 1985). As regards the volcanic activity, the onset in the NW sector (basaltic andesite) occurs during the deposition of the Ponte Gardena Conglomerate (Benciolini et al. 2001a; Brondi et al. 1970; Di Battistini et al. 1989; Krainer 1993), a discontinuous alluvial deposit of Upper(?) Carboniferous to Lower Permian age. Age data for the upper rhyolite are 276 Ma (fission track of the glass matrix; Storzer 1970), 276-272 Ma (Rb-Sr whole rock data; D'Amico & Del Moro 1988) and 260-255 Ma (palynostratigraphy in lacustrine sediments interbedded with rhyolitic ignimbrite; Barth & Mohr 1991; Cassinis & Doubinger 1991). Recent single-zircon U/Pb dating of acidic volcanic products from the western sector of the volcanic platform (Bargossi et al. 2004) provides new evidence for the earliest onset of acidic magmatism (284.9 ± 1.6 Ma) and is

[1] Dipartimento di Mineralogia e Petrologia, Universita', corso Garibaldi 37, 35137 Padova, Italy. E-mail: dario.visona@unipd.it
[2] CNR – Istituto di Geoscienze e Georisorse, c.so Garibaldi 37, 35137 Padova, Italy
[3] Dipartimento di Georisorse e Territorio, Università di Udine, via del Cotonificio 144, I-33100 Udine, Italy
[4] Research School of Earth Sciences, Australian National University, Canberra, ACT 0200, Australia

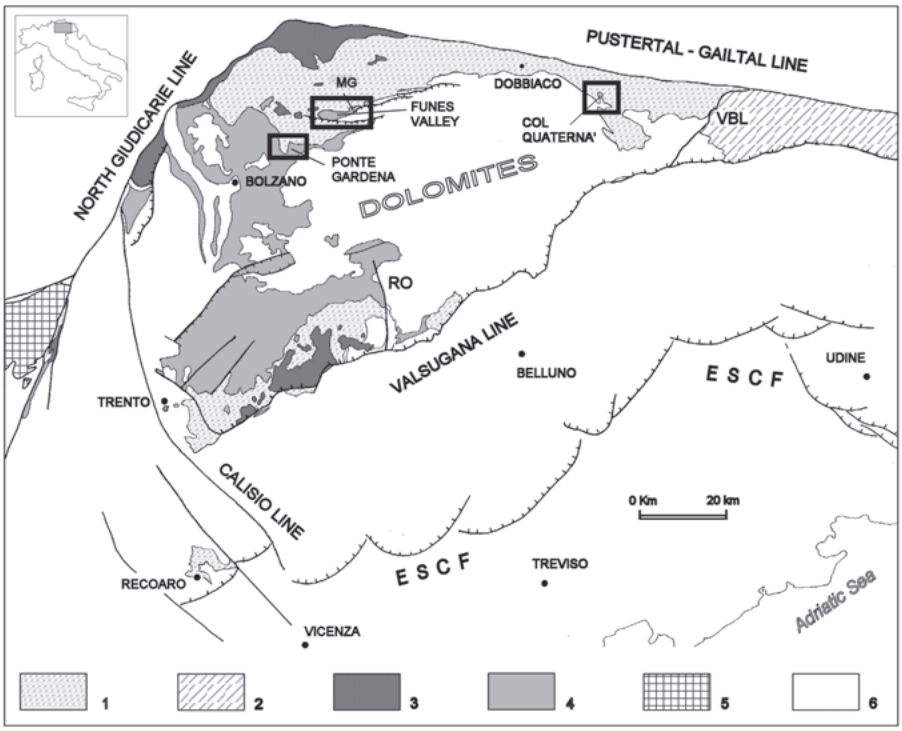

Fig. 1. Geological sketch of the Dolomite region. Legend: 1) Variscan metamorphic basement; 2) Paleocarnian Chain; 3) Early Permian intrusive bodies (Cima d'Asta, Bressanone-Chiusa, Ivigna, Monte Croce, Monte Sabion); 4) Athesian Volcanic District; 5) Tertiary intrusive body (Adamello); 6) Permo-Quaternary cover. MG: Monte dei Ginepri; VBL: Val Bordaglia Line; RO: Passo Rolle Line. ESCF: Eastern part of the Southern Alpine Chain Front.

consistent with the previous age of ca. 276 Ma for the main rhyolitic to rhyodacitic extrusive event.

This paper reports the geochronology of the NNW andesitic volcanism, which stratigraphically predates the main acidic event. Pristine andesite from the lowermost series, containing lenses of Ponte Gardena Conglomerate, was studied in order to define the age of onset of volcanism and to constrain the upper limit of the deposition of the conglomerate. An andesite neck (Monte dei Ginepri), which crosscuts the metamorphic basement and overlies mafic volcaniclastic deposits, was examined to further constrain the time span of mafic magmatism in the same area.

Lastly, the easternmost andesitic neck in the Eastern Southern Alps (Col Quaternà, about 80 km east of Monte dei Ginepri) was also investigated, with the aim of examining the polarity of the magmatism.

Geological setting

The study area belongs to the Eastern part of the Southern Alps Chain (ESC), a S-SE- verging, roughly WSW-ENE-trending fold-and-thrust belt, mostly Neogene in age, which developed at the north-eastern edge of the Apulian microplate (Doglioni & Bosellini 1987; Castellarin et al. 1992). The Periadriatic Lineament (Pustertal-Gailtal Line in Fig. 1) separates the ESC from the Austroalpine realm to the north. To the south, the Venetian Prealps mark the present front of the ESC, and to the west, the Giudicarie fault system separates the ESC from the Central Southern Alps (Fig. 1).

During Neogene compression, the crystalline basement was involved in the building of the ESC: today, it outcrops in the hanging-wall of the Valsugana Line, one of the most important structural lineaments of the ESC. This pre-Permian crystalline basement consists mostly of metapelitic and metapsammitic sequences of Early Paleozoic age, with interbedded felsic and mafic metavolcanic layers. To the east (Comelico and Western Carnian Alps), the silicoclastic sequences are first replaced by calc-schists and arenaceous marbles, and then by Silurian to Lower Devonian marbles (Zanferrari & Poli 1992). The Val Bordaglia Line separates the metamorphic basement from non-metamorphic sequences of the Paleocarnian Chain (Sassi et al. 1995). The ESC basement records greenschist-facies metamorphic conditions during the Variscan orogeny (thermal peak about 350 Ma) (Ring & Richter 1994, and references therein). An HT-LP metamorphism (sealed by the Brixen granodiorite pluton) has recently been documented at Colle dei Bovi (Benciolini et al. 2001b, 2006) and attributed to the Carboniferous orogenic collapse.

During the Late Carboniferous-Lower Permian, the Southalpine realm experienced intense magmatic activity (Bonin et al., 1993; Cortesogno et al. 1998). In particular, the Variscan crust, which now mostly outcrops in the hanging-wall of the Valsugana Line, was affected by both intrusive (Cima d'Asta, Bressanone, Ivigna, Monte Croce and Monte Sabion intrusions) and effusive magmatism (Athesian Volcanic District (AVD), and Monte Luco volcanics), which represent the major calc-alkaline association of Early Permian age.

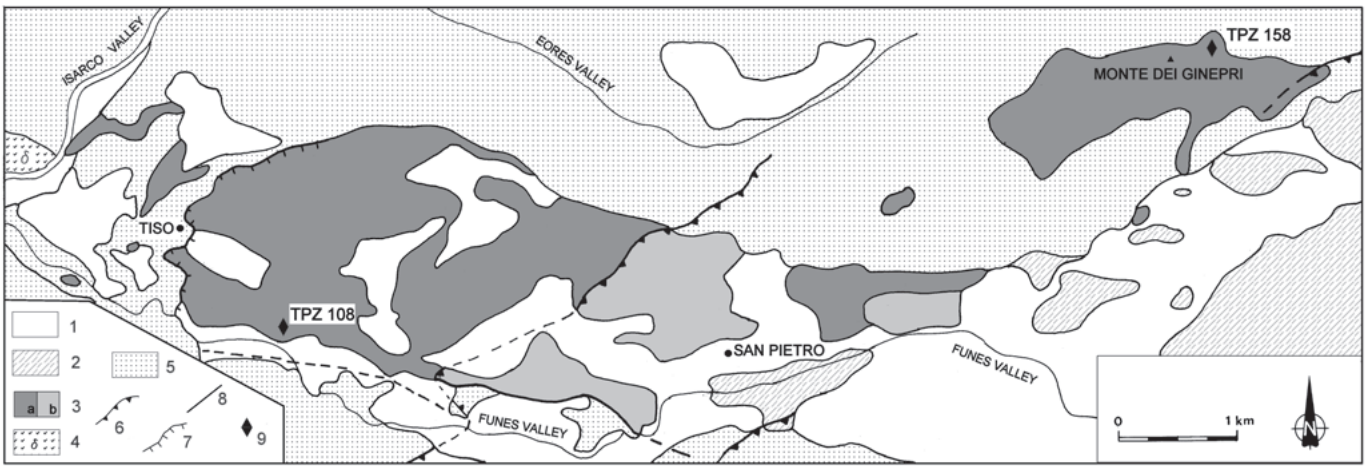

Fig. 2. Geological sketch map of Funes-Monte dei Ginepri area (location in Fig. 1). 1) Quaternary cover; 2) Upper Permian–Lower Triassic sedimentary cover; 3) Funes volcanic complex: a) Andesitic to basaltic-andesitic dykes, agglomerates; tuff; andesitic lava; Ponte Gardena conglomerates; b) Rhyolite and rhyodacite; 4) Chiusa Diorite; 5) Variscan metamorphic basement; 6) Neogene thrust; 7) Permian normal fault; 8) Fault; 9) Collected samples: TPZ 108 and TPZ 158 (after Benciolini et al., 2001a, and "Carta Geologica d'Italia", foglio 11 – M. Marmolada (II edition), 1970, scale 1:50.000.

According to Selli (1998), in the Dolomite area the AVD volcano-tectonic basin was bounded by four normal main paleolines: the Valsugana Line (south), Calisio Line (west), Funes valley Line (north) and, probably, Passo Rolle Line (east) (Fig. 1). This volcanic basin is subdivided into further basins and calderas, bounded by normal or transtensive faults which influenced the development of the magmatic basin in space and time (Benciolini et al. 2001a; Cassinis & Perotti 1993; Selli 1998).

On the basis of petrographic and geochemical characteristics, the Athesian Volcanic Complex is subdivided into two groups. The lower group comprises two distinct andesitic volcanic events (*basal andesitic event; upper andesitic event*), separated by an intermediate rhyodacitic event. The upper group is predominantly rhyodacitic-rhyolitic in composition (Bargossi et al. 1998; Selli 1998).

Alluvial to lacustrine clastic sediments, the composition of which reflects the siliciclastic and volcanic composition of the underlying basement, frequently alternate with lavas and tuffs. Jointly, they characterise the early Permian sequences of the Southalpine realm and reveal the activation of temporary alluvial or lacustrine environments during the volcanic activity (Collio and Tregiovo Fms.: Cassinis et al. 1997, Pedrunt unit: Benciolini et al. 2001a). The volcano-sedimentary Lower Permian cycle is topped by alluvial deposits of the Upper Permian Val Gardena Sandstone (Massari et al. 1994).

Two main hypotheses have been put forward regarding the geodynamic interpretation of the Early Permian volcanic cycle:

– dextral shear-zone with pull-apart basins (Arthaud & Matte 1977; Cassinis & Perotti 1993; Muttoni et al. 2003).
– continental rifting driven by crustal extension mechanisms (Dal Piaz & Martin 1996; Selli 1998).

Sample sites: stratigraphy and petrography

The stratigraphically older volcanic sequences outcropping at the northern margin of the AVD were sampled in the Funes valley and near Ponte Gardena, together with an andesitic neck that cuts the metamorphic basement on the left flank of the Eores valley (Monte dei Ginepri). The neck at Col Quaternà, located on the eastern tip of the Athesian platform, and recently assigned an Early Permian age on the basis of stratigraphic relationships (Poli 1997; Fig. 1), was also sampled.

Funes Valley

The volcano-sedimentary complex in this valley (Benciolini et al. 2001a; Fig. 2), lies on the low-grade metamorphic basement and is composed of andesitic blocky lava (maximum thickness 500 m) which, eastwards, changes rapidly into pyroclastic deposits interfingered with alluvial sediments. Meter-scale lenses of conglomerates and breccias with pebbles of the underlying basement (similar to the Ponte Gardena Conglomerate) are locally interbedded with these pyroclastic deposits. Basaltic andesitic dykes of low- to high-K orogenic andesite affinity, which are geochemically and petrographically comparable with the nearby dioritic epipluton of Chiusa (Di Battistini et al. 1989; Visonà et al. 1987), crosscut both the basement and volcanic sequence. Thrust over this volcano-sedimentary complex lies an Alpine tectonic unit, composed of rhyodacite and rhyolitic ignimbrite lying on a metamorphic basement (Benciolini et al. 2001a).

The sampled base of the andesitic blocky lava (TPZ 108, Fig. 2) is a volcanoclastic deposit. Under the microscope, the sample appears severely weathered and is made up of an indecipherable groundmass, with ghosts of rectangular phenocrysts (plagioclase?) and rare rounded quartz.

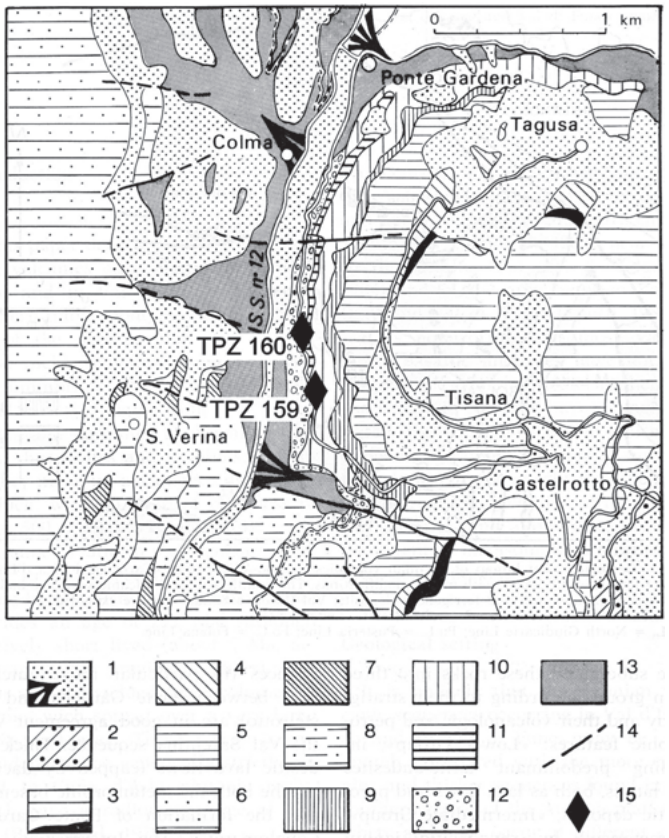

Fig. 3. Geological sketch of Ponte Gardena-Castelrotto area (slightly modified from Di Battistini et al., 1989). 1) Quaternary continental deposits. Alluvial fans; 2) Val Gardena sandstone; 3) Rhyolitic ignimbrite; 4) Volcaniclastic sediments; 5) Reddish-violet rhyodacitic ignimbrite; 6) Pinkish rhyodacitic ignimbrite; 7) Reworked tuff and volcanic breccias; 8) Rhyodacitic ignimbrite; 9) Block lava of dacitic composition; 10) Andesitic block lava; 11) Volcanoclastic sediments; 12) Ponte Gardena conglomerate; 13) Metamorphic basement; 14) Fault; 15) Collected samples: TPZ 159 and TPZ 160.

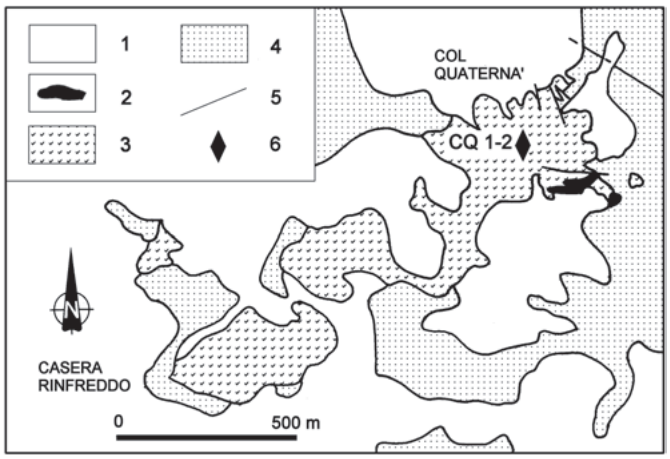

Fig. 4. Simplified geological map of Col Quaternà volcano-sedimentary complex (from Poli, 1997). Legend: 1) Quaternary deposits; 2) Ponte Gardena Conglomerate (Upper Carboniferous? – Lower Permian); 3) Andesitic body of Col Quaternà and pyroclastite; 4) Variscan metamorphic basement; 5) Fault; 6) Collected samples: CQ1 and CQ2.

Ponte Gardena

The andesitic blocky lava was sampled (TPZ 159-160, Fig. 3) in the classic geological section at Ponte Gardena (about 10 km south of Funes), along the road to Castelrotto. The blocky lava is locally replaced by lava flows containing volcanic blocks and explosion breccias, overlying the volcaniclastic sediments (Di Battistini et al. 1989). The andesite is a severely altered rock in which the porphyritic texture appears in the form of structural relics. Plagioclase is almost completely transformed to albite + sericite, epidote, and carbonate; pyroxenes and biotite (?) are replaced by chlorite, opaque minerals and carbonates; the fine-grained groundmass contains sericite, chlorite, feldspars, opaque minerals and quartz.

Monte dei Ginepri

Sample TPZ 158 was taken at an andesitic neck located on the northern flank of Monte dei Ginepri (Val di Eores, NE of Funes; Fig. 2). This NNE-SSW-striking neck crosscuts the low-grade metamorphic basement and is a deeply altered glomero-porphyritic rock with phenocrysts of sericitised plagioclase, chloritised pyroxene, isometric magnetite, rare flakes of red biotite. The sample contains a relic of corroded garnet (1.5 mm) with a corona of sericitised plagioclase on an indecipherable groundmass.

Col Quaternà

The Col Quaternà is a stratigraphically dated Lower Permian volcanic complex in the Carnian Alps, about 80 km east of Funes (Figs. 1, and 4; samples CQ 1, CQ 2). The composite andesitic neck cuts a volcanic and volcanoclastic sequence, which lies on (and is partly interbedded with) ruditic levels of the Ponte Gardena Conglomerate (Poli 1997). The volcanic rocks are composed of grey to pale-green fine-grained porphyritic andesite. They consist of sericitised plagioclase, chloritised pyroxene and/or amphibole, minor chloritised biotite phenocrysts, and a groundmass of sericitised plagioclase, chloritised pyroxene and/or amphibole, chlorite, sericite, calcite, leucoxene, opaque minerals and quartz; rare apatite and zircons are also found (Hubich & Loeschke 1995).

Analytical techniques

U–Pb dating was carried out on a sensitive high-resolution ion microprobe (SHRIMP II) at the Australian National University, Canberra, following the procedures of Compston et al. (1992). Cathodoluminescence imaging (CI) was used to distinguish internal structures of zircon, such as possibly older, inherited cores, from younger overgrowths. Spots for analysis were chosen avoiding cracks and inclusions. The final analyti-

Table 1. Zircon SHRIMP U-Pb-Th data for sample TPZ 159

Grain spot	U (ppm)	Th (ppm)	Th/U	$^{206}Pb^*$ (ppm)	$^{204}Pb/^{206}Pb$	f_{206} %	Total $^{238}U/^{206}Pb$	±	Total $^{207}Pb/^{206}Pb$	±	Radiogenic $^{206}Pb/^{238}U$	±	Age (Ma) $^{206}Pb/^{238}U$	±
1.1	286	198	0.69	11.4	0.000395	0.55	21.572	0.273	0.0565	0.0012	0.0461	0.0006	290.6	3.7
2.1	325	148	0.46	12.7	0.000266	0.52	22.018	0.271	0.0562	0.0011	0.0452	0.0006	284.9	3.5
3.1	368	164	0.45	14.7	0.000251	0.38	21.514	0.259	0.0552	0.0011	0.0463	0.0006	291.8	3.5
4.1	203	75	0.37	7.8	–	0.21	22.304	0.301	0.0536	0.0014	0.0447	0.0006	282.1	3.8
5.1	250	100	0.40	9.9	0.000348	0.50	21.830	0.282	0.0561	0.0014	0.0456	0.0006	287.3	3.7
6.1	344	166	0.48	13.8	0.000162	0.25	21.376	0.270	0.0542	0.0011	0.0467	0.0006	294.0	3.7
7.1	510	286	0.56	20.0	0.000236	0.26	21.863	0.260	0.0541	0.0009	0.0456	0.0005	287.6	3.4
8.1	706	395	0.56	28.8	0.000153	0.05	21.082	0.235	0.0527	0.0008	0.0474	0.0005	298.6	3.3
9.1	252	108	0.43	9.9	0.000238	0.35	21.866	0.281	0.0549	0.0014	0.0456	0.0006	287.3	3.7
10.1	304	127	0.42	12.3	0.000122	0.19	21.205	0.263	0.0538	0.0011	0.0471	0.0006	296.5	3.7
11.1	252	96	0.38	9.7	0.000236	0.68	22.311	0.289	0.0574	0.0013	0.0445	0.0006	280.8	3.6
12.1	289	114	0.39	11.4	0.000391	0.44	21.787	0.273	0.0556	0.0022	0.0457	0.0006	288.0	3.6
13.1	292	154	0.53	12.0	0.000464	0.33	20.816	0.261	0.0550	0.0012	0.0479	0.0006	301.5	3.8
14.1	370	145	0.39	15.0	0.000251	0.16	21.267	0.255	0.0535	0.0010	0.0469	0.0006	295.8	3.5
15.1	476	258	0.54	18.6	–	0.19	22.021	0.336	0.0535	0.0009	0.0453	0.0007	285.8	4.3
16.1	267	155	0.58	10.7	0.000272	0.24	21.455	0.273	0.0541	0.0012	0.0465	0.0006	293.0	3.7
17.1	251	137	0.54	10.1	0.000702	0.40	21.488	0.275	0.0553	0.0013	0.0464	0.0006	292.1	3.7
18.1	197	76	0.39	7.9	0.000108	0.54	21.336	0.288	0.0565	0.0015	0.0466	0.0006	293.7	4.0

Notes: 1. Uncertainties given at the one σ level.
2. Error in FC1 Reference zircon calibration was 0.40% for the analytical session (not included in above errors but required when comparing data from different mounts)
3. f_{206} % denotes the percentage of ^{206}Pb that is common Pb.
4. Correction for common Pb made using the measured $^{238}U/^{206}Pb$ and $^{207}Pb/^{206}Pb$ ratios following Tera and Wasserburg (1972) as outlined in Williams (1998)

cal data were treated as indicated below using Isoplot/Ex (Ludwig 1999) and are listed in Tab. 1. $^{206}Pb/^{238}U$ ages were used for grains younger than 1100 Ma, and $^{206}Pb/^{207}Pb$ ages for grains older than that value. Inferred crystallisation ages are calculated as weighted mean $^{238}U/^{206}Pb$ ages after correction for common Pb, assessed using the $^{207}Pb/^{206}Pb$ ratio and model values according to Cumming & Richards (1975). As the main aim of our work was to define the crystallisation age, most of the SHRIMP analyses focused on the external parts of zoned crystals.

U-Pb results

U-Pb-Th SHRIMP analysis was applied to zircons separated from two andesitic lava samples (TPZ 159, TPZ 160), one andesitic neck (TPZ 158) and one volcaniclastic rock (TPZ 108) from the north-western part of the AVD, and from one sample of the composite andesitic neck at Col Quaternà (CQ1-2) crosscutting a Lower Permian sequence of volcanic and volcaniclastic material.

Samples TPZ 159 and TPZ 160 (Ponte Gardena). Zircon grains from the two andesitic lavas are remarkably similar in size, shape and CI pattern (Fig. 5a, b). Their maximum size is around 250 microns. They are clear, colourless, euhedral, stubby crystals, with a general aspect ratio of 2:1, and some of them contain melt/fluid inclusions (and small apatite crystals). Most of them show continuous fine oscillatory magmatic zoning from core to rim. No obvious, discordant cores were detected in sample TPZ 160, whereas two possibly older cores were observed, but not measured, in sample TPZ 159. Zircons of both samples have similar, generally low, U (150-700 ppm) and Th (400-60 ppm) contents and uniform (0.4-0.7) Th/U ratios (Tabs. 1, 2).

Eighteen analyses carried out on **TPZ 159** zircon rims yield a single population of ages (Fig. 6) with a weighted mean of 290.7 ± 3 Ma (MSWD = 2.4, probability of fit 0.001). Two spots (11.1, 13.1) appear as statistical outliers. When these two points are removed from the age calculation, the weighted mean is 290.7 ± 2.8 Ma (MSWD = 1.6, probability of fit 0.054).

SHRIMP analyses carried out on eleven rims and one magmatic centre of **TPZ 160** zircon yield a homogeneous single population (Fig. 7) with a $^{206}Pb/^{238}U$ age of 289.0 ± 3 Ma (MSWD = 1.19, probability of fit 0.29).

Sample TPZ 158 (Monte dei Ginepri). Zircon grains separated from the andesitic neck are very similar in shape and size to those found in the andesitic lavas, except that CI images in TPZ 158 reveal grains with a large, rounded, inherited core with euhedrally zoned, discordantly overgrown magmatic rim (Fig. 5e). Similar zircon internal structures were described by Barth (1994) in the Buss andesitic lava and interpreted as relics of inherited crustal material, and thus evidence for magma contamination during the evolution.

The Th/U ratios of both cores (0.2-0.9) and rims (0.2-0.4) of zircon **TPZ 158** (Tab. 3) are similar to values reported in the

Table 2. Zircon SHRIMP U-Pb-Th data for sample TPZ 160

Grain spot	U (ppm)	Th (ppm)	Th/U	$^{206}Pb^*$ (ppm)	$^{204}Pb/^{206}Pb$	f_{206} %	Total $^{238}U/^{206}Pb$	±	Total $^{207}Pb/^{206}Pb$	±	Radiogenic $^{206}Pb/^{238}U$	±	Age (Ma) $^{206}Pb/^{238}U$	±
1.1	286	104	0.36	11.1	0.000461	0.31	22.057	0.278	0.0544	0.0012	0.0452	0.0006	285.0	3.6
2.1	293	171	0.58	11.3	0.000424	0.36	22.202	0.280	0.0549	0.0012	0.0449	0.0006	283.0	3.6
3.1	400	242	0.60	15.7	0.000259	0.06	21.822	0.306	0.0526	0.0010	0.0458	0.0007	288.7	4.0
4.1	342	282	0.82	13.6	0.000328	0.43	21.678	0.264	0.0556	0.0011	0.0459	0.0006	289.5	3.5
5.1	188	87	0.46	7.3	0.000762	0.65	21.991	0.406	0.0572	0.0015	0.0452	0.0008	284.9	5.2
6.1	184	69	0.37	7.4	0.000302	0.26	21.264	0.291	0.0543	0.0015	0.0469	0.0007	295.5	4.0
7.1	348	185	0.53	13.7	0.000441	0.53	21.764	0.265	0.0563	0.0015	0.0457	0.0006	288.1	3.5
8.1	155	59	0.38	6.1	0.000777	0.80	21.744	0.313	0.0585	0.0017	0.0456	0.0007	287.6	4.1
9.1	186	95	0.51	7.4	0.000590	0.58	21.636	0.298	0.0568	0.0017	0.0459	0.0006	289.6	4.0
10.1	412	183	0.44	16.7	0.000361	0.36	21.170	0.260	0.0552	0.0010	0.0471	0.0006	296.5	3.6
11.1	419	247	0.59	16.6	-	0.31	21.691	0.257	0.0546	0.0010	0.0460	0.0006	289.7	3.4

Notes as in Table 1.

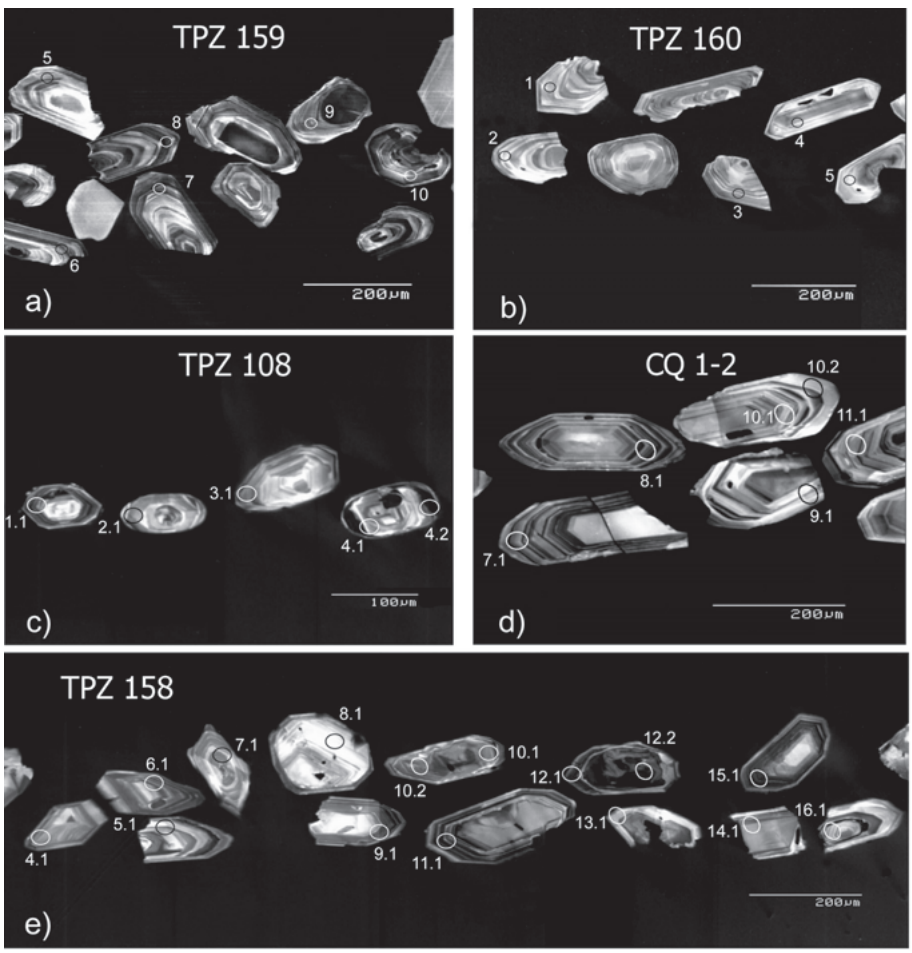

Fig. 5. Cathodoluminescence images of zircons from samples TPZ 159 (a); TPZ 160 (b); TPZ 108 (c), CQ1–2 (d), TPZ 158 (e). Circles: SHRIMP pits; numbers indicate analysed spots.

literature for magmatic zircons (Rubatto & Gebauer 1999). SHRIMP analyses carried out on seven cores (Tab. 3) yield three Paleoproterozoic (2041 ± 4, 1832 ± 22, 1802 ± 27 Ma), one Early Neoproterozoic (985.2 ± 15 Ma) and two Late Neoproterozoic (726.5 ± 9, 691.6 ± 7.1 Ma) ages. The age of 601.3 ± 7.5 Ma is significantly displaced from concordia (Fig. 8) and is difficult to assess, although it must be emphasised that the low level of ^{207}Pb may cause imprecise estimates of concordance in relatively young zircons. Analyses carried out on thirteen zircon rims yield ages ranging between 271.7 ± 3.4 and 288.8 ± 3.7

Table 3. Summary of SHRIMP U-Pb zircon results from sampleTPZ 158

Grain spot	U (ppm)	Th (ppm)	Th/U	$^{206}Pb^*$ (ppm)	$^{204}Pb/^{206}Pb$	f_{206} %	Total Ratios				Radiogenic Ratios						Age (Ma)				
							$^{238}U/^{206}Pb$	±	$^{207}Pb/^{206}Pb$	±	$^{206}Pb/^{238}U$	±	$^{207}Pb/^{235}U$	±	$^{207}Pb/^{206}Pb$	±	ρ	$^{206}Pb/^{238}U$	±	$^{207}Pb/^{206}Pb$	±	% Disc
1.1	103	69	0.67	8.7	–	0.23	10.205	0.130	0.0618	0.0010	0.0978	0.0013						601.3	7.5			
2.1	598	70	0.12	58.3	0.000022	0.18	8.814	0.093	0.0640	0.0005	0.1132	0.0012						691.6	7.1			
2.2	461	250	0.54	52.1	–	<0.01	8.384	0.111	0.0643	0.0005	0.1193	0.0016	1.059	0.016	0.0644	0.0005	0.853	726	9	754	17	4
3.1	463	69	0.15	17.9	0.000061	0.02	22.267	0.245	0.0521	0.0006	0.0449	0.0005						283.1	3.1			
4.1	239	67	0.28	9.3	0.000141	<0.01	21.970	0.260	0.0513	0.0009	0.0456	0.0005						287.2	3.4			
5.1	219	66	0.30	8.4	0.000175	0.06	22.423	0.273	0.0524	0.0010	0.0446	0.0005						281.1	3.4			
6.1	592	60	0.10	22.1	–	0.06	23.041	0.253	0.0522	0.0006	0.0434	0.0005						273.7	3.0			
7.1	430	75	0.18	16.5	0.000187	0.16	22.360	0.250	0.0532	0.0007	0.0447	0.0005						281.6	3.1			
8.1	70	62	0.88	5.2	0.000202	0.31	3.123	0.038	0.1147	0.0009	0.3192	0.0039	4.930	0.085	0.1120	0.0014	0.715	1786	19	1832	22	3
9.1	172	66	0.38	6.4	–	0.41	23.139	0.291	0.0550	0.0011	0.0430	0.0005						271.7	3.4			
10.1	236	60	0.26	3.0	0.000009	0.49	21.745	0.248	0.0560	0.0008	0.0458	0.0005						288.4	3.3			
10.2	254	49	0.19	4.7	–	0.39	21.739	0.284	0.0552	0.0011	0.0458	0.0006						288.8	3.7			
11.1	616	66	0.11	23.5	0.000070	<0.01	22.502	0.244	0.0518	0.0007	0.0444	0.0005						280.4	3.0			
12.1	740	149	0.20	3.8	0.010109	18.48	23.032	0.255	0.1985	0.0017	0.0354	0.0011						224.2	6.8			
12.2	891	61	0.07	266.9	0.000003	0.01	2.867	0.031	0.1259	0.0003	0.3488	0.0038	6.054	0.067	0.1259	0.0003	0.976	1929	18	2041	4	6
13.1	262	67	0.26	10.0	0.000164	0.50	22.426	0.262	0.0558	0.0009	0.0444	0.0005						279.9	3.2			
14.1	342	61	0.18	12.8	0.000050	0.17	22.861	0.312	0.0531	0.0008	0.0437	0.0006						275.5	3.7			
15.1	825	59	0.07	31.2	–	0.11	22.746	0.345	0.0527	0.0005	0.0439	0.0007						277.0	4.1			
16.1	268	63	0.24	38.1	0.000062	0.11	6.049	0.102	0.0718	0.0006	0.1651	0.0028	1.614	0.032	0.0709	0.0007	0.860	985	15	954	20	-3
17.1	64	62	0.97	17.4	0.000195	0.31	3.179	0.044	0.1128	0.0011	0.3136	0.0044	4.764	0.097	0.1102	0.0016	0.687	1758	22	1802	27	2

Notes as in Table 1.

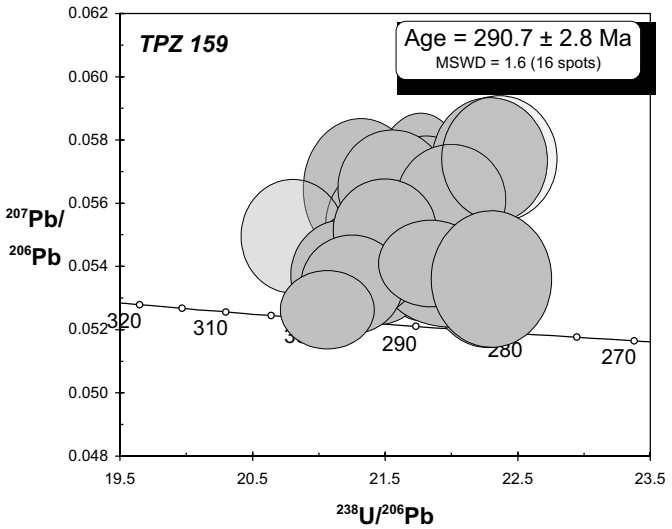

Fig. 6. Tera-Wasserburg diagram representing U-Pb data from sample TPZ 159. Error ellipses: 1σ error. Ages at 95% confidence level. Data plotted as paler ellipses were not used to calculate the main crystallisation age.

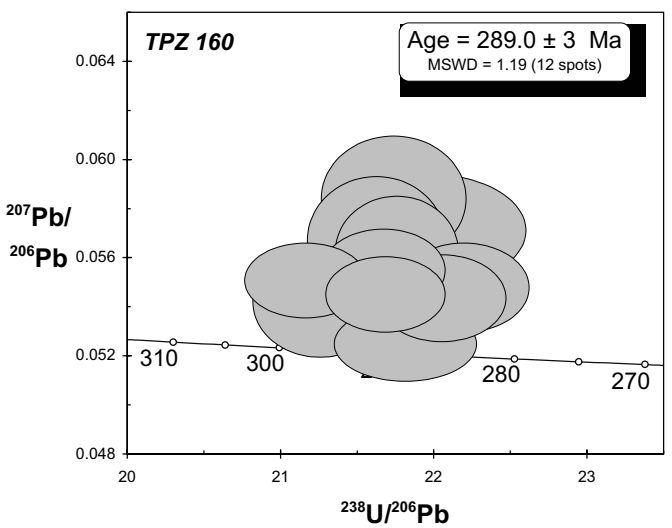

Fig. 7. Tera-Wasserburg diagram representing U-Pb data from sample TPZ 160. Error ellipses: 1σ error. Ages at 95% confidence level.

Ma (Tab. 3). An age of 224 ± 6.8 Ma was obtained on a grain (spot 12.1) showing a high common lead fraction (f_{206} = 18.48%), which probably indicates later interactions. For this reason, this point was excluded from age calculations. The weighted mean of the remaining twelve points yields a $^{206}Pb/^{238}U$ age of 280.7 ± 3.5 Ma, with a MSWD = 2.7, which appears too high for one single population. The probability density plot of the twelve spots (Fig. 9) does not show a simple Gaussian distribution and suggests more than one population. Three spots from two grains (4.1, 10.1, 10.2) yield a weighted mean of 288.1 ± 5.1 (MSWD=0.06). This old age is within error

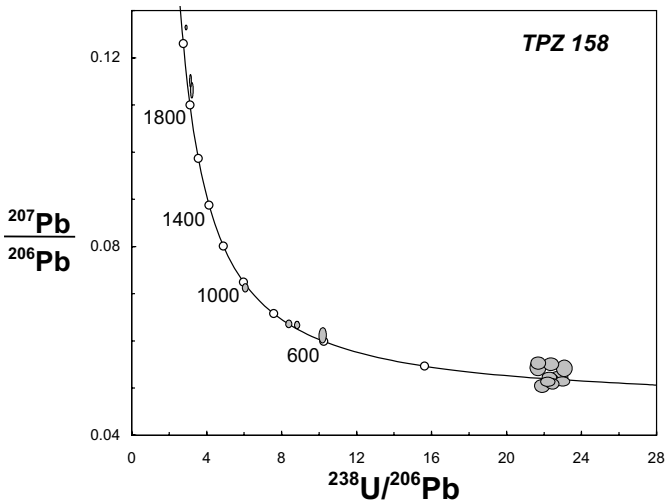

Fig. 8. Tera-Wasserburg diagram for U-Pb data from sample TPZ 158. Data plotted as paler ellipses were not used to calculate the main crystallisation age (see text for explanation).

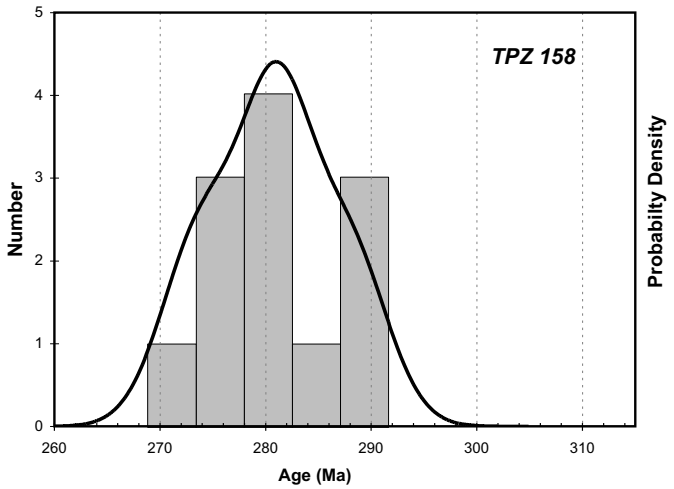

Fig. 9. Probability density plot of $^{206}Pb/^{238}U$ ages from sample TPZ 158. Histogram distribution indicates more than one age population. Two or three populations are possible.

Table 4. Zircon SHRIMP U-Pb-Th data for sample TPZ 108

Grain spot	U (ppm)	Th (ppm)	Th/U	$^{206}Pb^*$ (ppm)	$^{204}Pb/^{206}Pb$	f_{206} %	Total $^{238}U/^{206}Pb$	±	Total $^{207}Pb/^{206}Pb$	±	Radiogenic $^{206}Pb/^{238}U$	±	Age (Ma) $^{206}Pb/^{238}U$	±
1.1	568	430	0.76	61.5	0.000068	2.48	7.939	0.087	0.0846	0.0015	0.1228	0.0015	746.9	8.4
2.1	292	121	0.41	28.1	0.000147	0.20	8.929	0.096	0.0639	0.0005	0.1118	0.0012	683.0	7.2
3.1	377	29	0.08	24.6	0.000262	0.18	13.135	0.142	0.0580	0.0006	0.0760	0.0008	472.1	5.0
4.1	462	185	0.40	52.7	0.000119	0.46	7.523	0.082	0.0696	0.0005	0.1323	0.0015	801.1	8.4
4.2	593	143	0.24	68.9	0.000018	0.05	7.402	0.077	0.0667	0.0003	0.1350	0.0014	816.5	8.2

Notes as in Table 1.

of the age of the andesite country rocks, suggesting that these two grains may represent xenocrysts from the intruded lava (TPZ 159, TPZ 160) or were inherited from the magma chamber. The weighted mean of the remaining 9 spots yields an age of 278.4 ± 3.9 Ma (MSWD = 1.5, probability of fit = 0.16). The spread of this population is still higher than a normal distribution and may indicate further complexity. Results of the unmix calculation made with Isoplot suggest two populations, with a relative misfit of 0.976 (Fig. 9). The younger population, at 274.2 ± 4.2 Ma, may result from minor Pb loss. The second population yields an age of 280.2 ± 3.6 Ma, which we interpret as the emplacement age of the neck (final errors include error in the standard). In either case, whether the best estimate of the emplacement age is 278.4 ± 3.9 or 280.2 ± 3.6 Ma, these ages (within error of each other) show that the andesitic neck is slightly younger than the andesitic lava flows it intruded, consistent with field relationships.

Sample TPZ 108 (Tiso). Only a few zircon grains were recovered from this volcaniclastic sample. Zircons range from euhedral crystals with rounded tips to rounded grains. Their CI reveals distinct internal structures (Fig. 5c). Some grains show continuous, fine, oscillatory zoning from core to rim; others have luminescent, zoned cores and darker euhedrally zoned rims; yet others have irregularly zoned cores and dark overgrowths.

U-Pb-Th SHRIMP analysis was carried out on five rims of four crystals (Tab. 4). The Tera-Wasserburg plot (Fig. 10) shows that two analyses are highly discordant and yield $^{206}Pb/^{238}U$ ages of 801.1 ± 8.4 and 746.9 ± 8.4 Ma. Two other points are slightly above the concordia line and have $^{206}Pb/^{238}U$ ages of 683 ± 7.2 and 472.1 ± 5 Ma. Only one point touches the concordia line at 816.5 ± 8.2 Ma, an early Pan-African age, which is quite common in the Variscan crustal basement of Central Europe (Gebauer, 1993). All grains except one have Th/U ratios between 0.25 and 0.80, typical of magmatic zircon. The 472.1 ± 5 Ma zircon shows a much lower ratio (0.08), which is more typical of metamorphic zircons. None of the grains provides the age of the extrusive event.

Sample CQ1-2 (Col Quaternà). Zircon grains from the andesitic neck of Col Quaternà have a maximum size of around

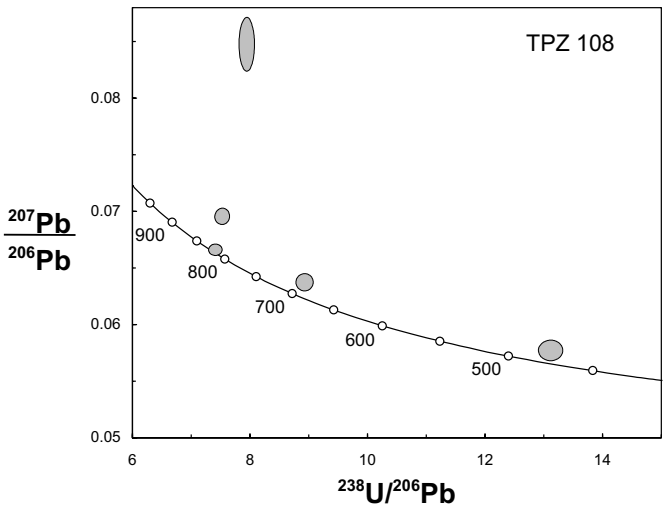

Fig. 10. Tera-Wasserburg diagram representing U-Pb data from sample TPZ 108.

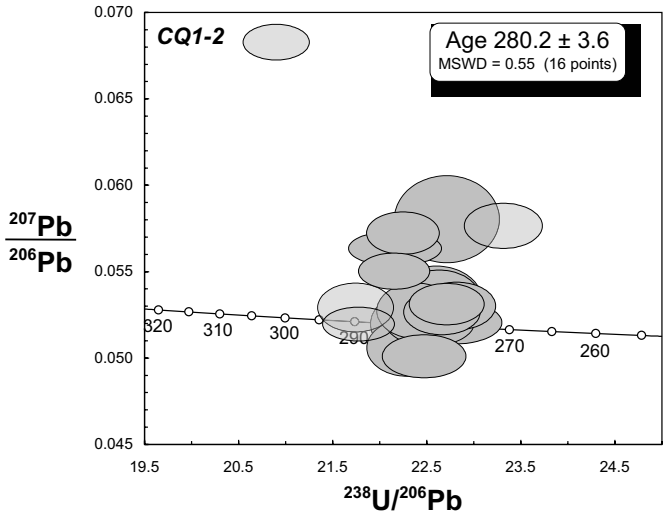

Fig. 11. Tera-Wasserburg diagram for analysed zircon spots from sample CQ-1-2. Data plotted as paler ellipses were not used to calculate the main crystallisation age (see text for explanation).

Table 5. Zircon SHRIMP U-Pb-Th data for sample CQ 1-2

Grain spot	U (ppm)	Th (ppm)	Th/U	^{206}Pb* (ppm)	^{204}Pb/ ^{206}Pb	f_{206} %	Total ^{238}U/ ^{206}Pb	±	Total ^{207}Pb/ ^{206}Pb	±	Radiogenic ^{206}Pb/ ^{238}U	±	Age (Ma) ^{206}Pb/ ^{238}U	±
2.1	232	77	0.33	8.6	0.000495	0.73	23.30	0.27	0.0575	0.0009	0.0426	0.0005	269.0	3.1
15.1	122	41		4.6	0.002062	0.76	22.70	0.36	0.0579	0.0017	0.0437	0.0007	275.8	4.4
3.1	233	64	0.28	8.8	0.000222	0.12	22.80	0.27	0.0528	0.0009	0.0438	0.0005	276.4	3.3
13.1	294	64	0.22	11.1	0.000059	<0.01	22.77	0.34	0.0518	0.0008	0.0439	0.0007	277.0	4.0
12.1	319	63	0.20	12.1	–	0.13	22.70	0.26	0.0529	0.0008	0.0440	0.0005	277.6	3.2
10.2	254	66	0.26	9.6	–	0.07	22.65	0.27	0.0524	0.0009	0.0441	0.0005	278.3	3.3
3.2	166	65	0.39	6.3	0.000074	0.17	22.62	0.29	0.0532	0.0011	0.0441	0.0006	278.4	3.5
11.1	215	75		8.2	0.000105	0.15	22.59	0.32	0.0530	0.0014	0.0442	0.0006	278.8	3.9
14.1	274	62	0.23	10.4	–	<0.01	22.52	0.31	0.0517	0.0009	0.0444	0.0006	280.1	3.8
6.1	200	62	0.31	7.6	0.000085	<0.01	22.46	0.29	0.0517	0.0014	0.0445	0.0006	280.8	3.5
1.1	257	70	0.27	9.8	–	<0.01	22.46	0.29	0.0498	0.0009	0.0446	0.0006	281.5	3.6
4.1	226	60	0.27	8.7	–	0.07	22.38	0.27	0.0525	0.0011	0.0447	0.0005	281.6	3.4
5.2	251	79	0.32	9.7	0.000623	0.64	22.24	0.25	0.0571	0.0008	0.0447	0.0005	281.8	3.2
2.2	224	64	0.29	8.6	–	<0.01	22.31	0.27	0.0517	0.0012	0.0448	0.0005	282.8	3.4
4.2	348	152	0.44	13.5	0.000163	0.53	22.15	0.32	0.0562	0.0007	0.0449	0.0007	283.1	4.1
9.1	151	66	0.44	5.8	–	<0.01	22.29	0.28	0.0503	0.0011	0.0450	0.0006	283.5	3.6
5.1	317	90	0.28	12.3	0.000245	0.35	22.15	0.25	0.0548	0.0007	0.0450	0.0005	283.7	3.1
8.1	366	74	0.20	14.5	0.000154	<0.01	21.77	0.25	0.0517	0.0007	0.0460	0.0005	289.6	3.2
10.1	214	69	0.32	8.5	–	0.07	21.74	0.26	0.0527	0.0010	0.0460	0.0006	289.7	3.5
7.1	466	66	0.14	19.1	–	2.01	20.91	0.23	0.0684	0.0007	0.0469	0.0005	295.3	3.3

Notes as in Table 1.

250 microns, and a general aspect ratio of 2.5. They are clear, and include several melt (and fluid) inclusions.

In most grains, CI reveals continuous, fine, oscillatory magmatic zoning from core to rim. Obvious discordant cores were not observed (Fig. 5d). U-Pb-Th analysis on rims and cores show extremely uniform Th/U ratios, typical of magmatic zircons, and yield ages ranging between 275.8 ± 4.4 and 289.7 ± 3.5 Ma (Tab. 5, Fig. 11). One younger age of 269.0 ± 3.1 Ma (core) is suspected to have undergone Pb loss, whereas the older age of spot 7.1 (295.3 ± 3.3 Ma) is probably affected by the higher (f_{206} = 2.01%), common Pb content, or represents an inherited grain, as probably do the two second older ages of 289.7 and 289.6 Ma (spots 8.1 and 10.1). These four analyses were excluded from age calculations. The remaining sixteen

data points (both centres and rims) give a weighted mean age of 280.2 ± 3.6 Ma (MSWD = 0.55), which we interpret as the best estimate of the age of andesitic magmatism in the north-easternmost sector of the AVD.

Discussion

The andesite overlying the Ponte Gardena Conglomerate (samples TPZ 159 and 160) contains stubby euhedral zircon crystals. Their ages of 290.7 ± 3 Ma and 289.0 ± 3 Ma, respectively, are interpreted as magmatic. Although these ages are identical within error, the slightly younger age of TPZ 160 is consistent with its higher stratigraphic position (50 m). Zircon ages from the Monte dei Ginepri andesitic neck (TPZ 158), located just NE of the Tiso basin, show a bimodal, or possibly tri-modal distribution (Fig. 9), unlike those observed in the other data sets. This distribution suggests a more complex, albeit speculative, interpretation. The first group of three older grains yields an age of 288.1 ± 5.1 Ma. This older zircon age is identical, within error, to the age of the andesitic lava and suggests that this zircon population is an inherited component from country rocks or the magma chamber. The emplacement age of the neck is estimated at 278.4 ± 3.9 Ma (or 280.2 ± 3.6; see U-Pb results section). Zircons from the Col Quaternà neck show typical magmatic features and lack inherited cores. Sixteen spots (at both centres and borders) yield a weighted mean age of 280.2 ± 3.6 Ma (MSWD = 0.55), which is interpreted as the best estimate of the age of andesitic magmatism in the north-easternmost sector of the AVD. This age is identical, within error, to that of the Monte dei Ginepri neck.

Two episodes of andesitic lava flow production, separated by a more acidic event, are clearly described from the central and southern parts of the AVD (Bargossi et al., 1998). The age of the acidic event (284.9 ± 1.6 Ma) (Bargossi et al. 2004) is intermediate between the age of the lower andesite lava flows at Ponte Gardena and that of the late andesite necks at Monte dei Ginepri and Col Quaternà which, in turn, have the same age as the uppermost andesitic lava (278.4 ± 1.5 Ma) from the western part of the AVD (Bargossi et al. 2004). This is consistent with the existence of two distinct andesitic pulses about 10 Ma apart.

Older ages have been found for the detrital zircons of volcaniclastic deposits in the Funes basin at the bottom of the basal andesite (TPZ 108) and in inherited zircon cores from the Monte dei Ginepri andesitic neck (TPZ 158). It must be emphasised that, as this work has focused on dating magmatic crystallisation ages, these instances cannot be taken as fully representative of the age or degree of inheritance in the volcanic rocks.

In the case of the Funes basin volcaniclastic deposit, the zircons are detrital grains of both magmatic and metamorphic origin. The rims of three crystals give a concordant age of 816.5 ± 8.2 Ma and two other ages, slightly above the concordia line, of 683 ± 7.2 and 472.1 ± 5 Ma.

This latter age of 472.1 ± 5 Ma of one grain from volcaniclastic sample TPZ 108 is within error with the 479 ± 8 Ma age obtained for the Lower Paleozoic magmatism of the Southalpine domain (Comelico porphyroids, Meli & Klötzli 2001). It is therefore reasonable to assume that this grain may derive from the erosion of the Paleozoic porphyroid part of the crystalline basement, on which the volcaniclastic sequence now rests.

As regards the remaining detrital zircons and inherited cores, their ages are similar to those in other Alpine areas, e.g., Tauern Window (Eastern Alps, Eichhorn et al. 2001), Ivrea Zone (Central Alps, Vavra et al. 1996) and Betic Rift Belt (Zeck & Whitehouse 1999; Zeck & Williams 2001). The Paleoproterozoic-Pan-African zircon age patterns generally correspond to those established for the Hercynian basement in Southern Europe, which is considered to be reworked Gondwana crust. This observation fits recent paleomagnetic data on the volcanic deposits lying on the northern margin of Gondwana (Pangea "B"; Muttoni et al. 2003).

Conclusions

- Magmatic zircon dating from the Ponte Gardena andesite magma yields a $^{206}Pb/^{238}U$ age of 290.7 Ma, testifying to the oldest volcanic activity yet documented in the AVD.
- Ages obtained from the andesitic necks of Monte dei Ginepri and Col Quaternà, (278.4 ± 3.9, 280.2 ± 3.6 Ma), are significantly younger and indicate a second magmatic pulse, some 10 Ma later. Two pulses appear to be a quite widespread phenomenon, as two events of andesite lava flows have been reported (Bargossi et al. 1998) also in the central and southern sectors of the Athesian platform. Unlike the coeval plutonic magmatism, there is no evidence, at present, for a space-time polarity of the extrusive events.
- The $^{206}Pb/^{238}U$ zircon age from Col Quaternà is consistent with its Lower Permian age, attributed on the basis of stratigraphic relationships (Poli 1997).
- The lowermost volcanoclastic deposit of the Funes valley volcano-sedimentary complex contains detrital zircons only, one grain of which (472.1 ± 5 Ma) probably derives from erosion of Paleozoic porphyroids. Other zircons from the same volcaniclastic sediments and inherited cores of magmatic zircons from andesite give Paleoproterozoic, Early Neoproterozoic and Late Neoproterozoic ages. These ages are typical of the Africa domain and fit the model, according to which the Dolomitic region was still part of Gondwana during the Proterozoic and Neoproterozoic.

Acknowledgements

The research was sponsored by M.U.R.S.T. grant (COFIN 1997). We are grateful to the Editor M. Engi and to the anonymous referee for their constructive comments.

REFERENCES

Arthaud, F., & Matte, Ph. 1977: Late Paleozoic strike-slip faulting in southern Europe and northern Africa: result of a right-lateral shear zone between the Appalachians and the Urals. Geological Society of America, Bulletin 88, 1305–1320.

Bargossi, G.M., Rottura, A., Vernia, L., Visonà D., & Tranne C.A. 1998: Guida all'escursione sul distretto vulcanico atesino e sulle plutoniti di Bressanone-Chiusa e Cima d'Asta. Memorie della Società di Geologia Italiana 53, 23–41.

Bargossi G.M., Klötzli U. S., Mair V., Marocchi M. & Morelli C. 2004: The Lower Permian Athesian volcanic group (AVG) in the Adige Valley between Merano and Bolzano: a stratigraphic, petrographic and gechronological outline. Abstract, 32nd IGC Congress, Florence.

Barth, S. 1994: Calc-alkaline basic to silicic rock suites from the Late Hercynian Atesina-Cima d'Asta volcano-plutonic complex (Southern Alps, N. Italy): Evidence for primary magmatic and hydrothermal alteration processes. Neues Jahrbuch für Mineralogie, Abhandlungen 168, 15–46.

Barth, S. & Mohr, B. 1991: Late Hercynian magmatism in the Southern Alps, N. Italy: Oxygen isotope data of the Atesina volcanic complex Cima d'Asta intrusion and palynological age of lacustrine sediments from Tregiovo. EUG VI Strasbourg, Terra Cognita 3, 209–210 (abstract).

Benciolini, L., Poli, M.E., Visonà, D. & Zanferrari, A. 2001: The Funes/Villnöss basin: an example of early Permian tectonics, magmatism and sedimentation in the Eastern Southern Alps (NE Italy). "NATURA BRESCIA-NA", Annali del Museo Civico di Scienze Naturali di Brescia 25, 133–138.

Benciolini, L., Poli, M.E., Visona', D. & Zanferrari, A. 2001b: Pressure temperature time path of the Col dei Bovi metamorphic unit (Eastern Southalpine Basement, South Tyrol). Geologisch-Palaeontologische Mitteilungen Innsbruck 25, 25–26.

Benciolini, L., Poli, M.E., Visona', D. & Zanferrari, A. 2006: Looking inside Late Variscan tectonics: structural and metamorphic heterogeneity of the Eastern Southalpine Basement (NE Italy). Geodinamica Acta 19, 17–32.

Bonin, B., Brandlein, P., Bussy, F., Desmons, J., Eggenberger, U., Finger, F., Graf, K., Marro, C., Mercolli, I., Oberhänsli, R., Ploquin, A., Von Quadt, A., Von Raumer, J., Schaltegger, U., Steyrer, H.P., Visona', D. & Vivier, G. 1993: Late Variscan Magmatic Evolution of the Alpine Basement. In: J. von Raumer & F. Neubauer (eds.), Pre-Mesozoic Geology in the Alps. Springer-Verlag, Heidelberg, pp. 169–199.

Brondi, A., Ghezzo, C., Guasparri, G., Ricci, C.A. & Sabatini, G. 1970: Le vulcaniti Paleozoiche nell'area settentrionale del complesso effusivo atesino. Nota I – Successione stratigrafica, assetto strutturale e vulcanologico nella Val Sarentina. Atti della Società Toscana di Scienze Naturali, Memorie, Serie A 77,157–200.

Cassinis, G., & Doubinger, J. 1991: On the geological time of the typical Collio and Tregiovo continental beds in the Southalpine Permian (Italy), and some additional observations. Atti Ticinensi di Scienze della Terra 34, 1–20.

Cassinis, G., & Perotti, C. 1993: – Interazione strutturale permiana tra la linea delle giudicarie e i bacini di Collio, Tione e Tregiovo (Sudalpino Centrale, N-Italia). Bolletino della Società geologica italiana 112, 1021–1036.

Cassinis, G., Perotti, C. & Venturini, C. 1997: Examples of late Hercynian transtensional tectonics in the Southern Alps (Italy). In: J.M. Dickins (ed.), Late Palaeozoic and Early Mesozoic Circum-Pacific Events and Their Global Correlation. Cambridge University Press, 41–50.

Castellarin, A., Cantelli, L., Fesce, A.M., Mercier, J.L., Picotti, V., Pini, G.A., Prosser, G., & Selli, L. 1992: Alpine compressional tectonics in the Southern Alps. Relationships with the N. Appenines. Annales Tectonicae 6, 62–94.

Compston, W., Williams, I. S., Kirschvink, J. L., Zhang, Z. & Ma, G. 1992: Zircon U–Pb ages from the early Cambrian time-scale. Journal of the Geological Society of London 149, 171–184.

Cortesogno, L., Cassinis, G., Dellagiovanna, G., Gaggero, L., Oggiano, G., Ronchi, A., Seno, S., & Vanossi, M. 1998: The Variscan post-collisional volcanism in Late Carboniferous-Permian sequences of the Ligurian Alps, Southern Alps and Sardinia (Italy): a synthesis. Lithos, 45, 305–328.

Cumming, G. L. & Richards, J. R. 1975: Ore lead isotope ratios in a continuously changing Earth. Earth and Planetary Science Letters 28, 155–171.

Dal Piaz, G.V. & Martin, S. 1996: Evoluzione litosferica e magmatismo nel dominio Austro-Sudalpino dall'orogenensi varisica al rifting mesozoico. Memorie della Società di Geologia Italiana 53, 43–62.

D'amico, C., & Del Moro, A. 1988: Permian and Triassic Rb-Sr dating in the Pemian rhyodacitic ignimbrites of Trentino (Southern Alps). Rendiconti della Società Italiana de Mineralogia e Petrologia 43, 171–180.

Del Moro, A., & Visona', D. 1982: The epiplutonic Hercynian Complex of Bressanone (Brixen, Eastern Alps, Italy). Petrologic and radiometric data: Neues Jahrbuch für Mineralogie, Abhandlungen 145, 66–85.

Di Battistini, G., Gallo, F., Giammetti, F. & Vernia, L. 1989: Permian andesites from Val d'Isarco and Val di Funes volcanic sequence (Bolzano, northern Italy). Mineralogica et petrographica acta XXXII, 123–137.

Doglioni, C. & Bosellini, A. 1987: Eoalpine and mesoalpine tectonics in the Southern Alps. Geologische Rundschau 76, 735–754.

Eichhorn, R., Loth, G. & Kennedy, A. 2001: Unravelling the pre-Variscan evolution of the Habach terrane (Tauern Window, Austria) by U-Pb SHRIMP zircon data. Contributions to Mineralogy and Petrology 142, 147–162.

Gebauer, D. 1993: The pre-Alpine evolution of the continental crust of the Central Alps – an overview. In: Pre-Mesozoic Geology in the Alps, J. von Raumer & F. Neubauer (eds.), pp. 93–118.

Hubich, D., & Loeschke, J. 1995: Petrographie und Geochemie von Intrusivgesteinen der westlichen Karnischen Alpen (Obstanser See – Passo Silvella, Österreich/Italien. Jahrbuch der Geologie B.-A. 138, 309–319.

Krainer K. 1993: Late and post-Variscan sediments of the Eastern and Southern Alps. In: Pre-Mesozoic Geology in the Alps, J. von Raumer & F. Neubauer (eds.), pp. 537–565.

Ludwig, K. R. 1999: Isoplot/Ex 2.01: A geochronological toolkit for Microsoft Excel. Berkeley Geochronology Center Special Publication 1a, 50 pp.

Massari F., Neri C., Pittau P., Fontana D., & Stefani C. 1994: Sedimentology, palynostratigraphy and sequence stratigraphy of a continental to shallow-marine rift-related succession: the Upper Permian of the Eastern Southern Alps (Italy). Memorie di Scienze Geologiche di Padova 46, 119–243.

Meli, S. & Klötzli, U.S. 2001: Evidence for Lower Paleozoic magmatism in the Eastern South-Alpine basement: zircon geochronology from Comelico porphyroids. Schweizerische Mineralogische und Petrographische Mitteilungen 81, 147–157.

Muttoni, G., Kent, D., Garzanti, E., Brack, P., Abrahamsen, N., & Gaetani, M. 2003: Early Permian Pangea 'B' to Late Permian Pangea 'A'. Earth and Planetary Science Letters 215, 379–394.

Poli, M.E. 1997: Età permiana inferiore del complesso vulcanico di Col Quaternà (Comelico, NE Italy). Atti Ticinesi di Scienze della Terra (Ser. spec.) 5, 53–64.

Ring, U. & Richter, C. 1994: The Variscan structural and metamorphic evolution of the eastern Southalpine basement. Journal of the Geological Society of London 151, 755–766.

Rottura, A., Bargossi, G.M., Caggianelli, A., Del Moro, A., Visona', D. & Tranne, C.A. 1998: Origin and significance of the Permian high-K calc-alkaline magmatism in the central-eastern Southern Alps, Italy. Lithos 45: 329–348.

Rubatto, D., & Gebauer, D. 1999: Use of cathodoluminescence for U–Pb zircon dating by ion microprobe: some examples from the Western Alps. In: Pagel, M., Barbin, V., Blanc, P. & Ohnenstetter, D. (eds.), *Cathodoluminescence in Geosciences*. Berlin: Springer, pp. 373–400.

Sassi R., Arkai P., Lantai C. & Venturini C. 1995: Location of the boundary between the metamorphic Southalpine basement and the Paleozoic sequences of the Carnian Alps: illite "cristallinity" and vitrinite reflectance data. Schweizerische Mineralogische und Petrographische Mitteilungen 75, 399–412.

Sassi, F.P., Cavazzini, G. & Visonà, D. 1985: Radiometric geochronology in the eastern Alps: results and problems. Rendiconti della Società Italiana de Mineralogia e Petrologia 40, 187–224.

Selli, L. 1998: Il lineamento della Valsugana fra Trento e Cima d'Asta: cinematica neogenica ed eredità strutturali permo mesozoiche nel quadro evolutivo del Sudalpino orientale (NE Italia). Memorie della Societa di Geologia Italiana 53: 503–541.

Storzer, D. 1970: Fission track dating of volcanic glasses and the thermal history of rocks. Earth and Planetary Science Letters 8, 55–60.

Vavra, G., Gebauer, D. & Schmid, R. 1996: Multiple zircon growth and recrystallization during polyphase Late Carboniferous to Triassic metamorphism in granulites of the Ivrea Zone (Southern Alps): an ion microprobe (SHRIMP) study. Contributions to Mineralogy and Petrology 122, 337–358.

Visonà, D., Alberti, F., Stefani, C. & Stenico, L. 1987: Le plutoniti di Chiusa, Dosso Lives e Luson. Una serie calc-alcalina Ercinica nelle Alpi Orientali. Memorie di Scienze Geologiche di Padova, XXXIX: 85–99.

Zanferrari A. & Poli M.E. 1992: Il basamento sudalpino orientale: stratigrafia, tettonica varisica e alpina, rapporti copertura-basamento. Studi Geologici Camerti, special volume 1992/2 CROP 1–1A, 299–302.

Zeck, H.P. & Whitehouse, M.J. 1999: Hercynian, Pan-African, Proterozoic and Archean ion-microprobe zircon ages for a Betic Rift core complex. Alpine belt, W Mediterranean – consequences for its *P-T-t* path. Contributions to Mineralogy and Petrology 134, 134–149.

Zeck, H.P. & Williams, I.S. 2001: Hercynian metamorphism in the Nappe Core Complex of the Alpine Betic Rift Belt, Western Mediterranean – a SHRIMP zircon study. Journal of Petrology 42, 1373–1385.

Manuscript received February 13, 2006
Revision accepted November 4, 2006
Published Online First July 20, 2007
Editorial handling: Martin Engi, Edwin Gnos